Geometrical Process Modeling and Simulation of Concrete Machining Based on Delaunay Tessellations

Nils Raabe[1], Christian Rautert[2], Manuel Ferreira[3], and Claus Weihs[1]

***Abstract*—Up to now tools used for machining of concrete are in general not adapted to the particular machining processes. As in mass production tool wear and production time are very cost sensitive factors, filling this lack is of great interest. This paper proposes a geometrical simulation model describing the forces affecting the workpiece as well as the chip removal rate and the wear rate of the used diamond in dependency of the process parameters. On the long run this model will help in determining the optimal process parameter settings in situations where material and hole diameters are given.**

Because the machined materials are in general abrasive usual discretized simulation methods like Finite Elements Models are inappropriate for describing the process behavior. In contrast, our approach assumes both material and diamond grain as tessellations of microparts connected by predetermined breaking points. The process is then iteratively simulated where in each iteration the forces are computed by interpreting the collisions of pairs of workpiece and grain microparts as force impacts.

After fitting the model to a series of real experiments based on a Statistical Design of Experiments the model is shown to reflect the real process behaviour very well.

***Index Terms*—numerical simulation, machining, DOE, regression analysis.**

I. Introduction

TOOL wear and machining time represent two dominant cost factors in cutting processes. To obtain durable tools with increased performance these factors have to be optimized, which demands the investigation of the interactions between tool and workpiece. Unlike ductile materials such as steel, aluminum or plastics, material characteristics for mineral substrates like concrete are difficult to determine due to their strongly inhomogeneous components, the dispersion of the aggregates and porosities, the time dependancy of the compression strength etc. (see [5]). As a result of the brittleness of mineral materials and the corresponding discontinuous chip formation, there are varying engagement conditions of the tool which leads to alternating forces and spontaneous tool wear by diamond fracture.

Despite the manifold of concrete specifications, tools for concrete machining are still more or less standardized tools which are not adapted to the particular machining application. The following analysis is carried out in a subproject of the Collaborative Research Center SFB 823. In non-percussive cutting of mineral subsoil such as trepanning, diamond impregnated sintered tools dominate the field of machining of concrete because of the diamonds' mechanical properties. These composite materials are fabricated powdermetallurgically. Well-established techniques like cold pressing with a following vacuum sintering process or hot-pressing, which is a very productive manufacturing route, are used for industrial mass production. The described powdermetallurgical fabrication process implies a statistical dispersion of the the diamonds embedded in the metal matrix. Additionally, the composition and allocation of different hard phases, cement and natural stone grit in the machined concrete are randomly distributed. Because of these facts, the exact knowledge of the machining process is necessary to be able to investigate for appropriate tool design and development.

To obtain a better understanding of these highly complex grinding mechanisms of inhomogeneous materials, which can not be described by physical means, statistical methods are used to take into account the effect of diamond grain orientation, the disposition of diamonds in the metal matrix and the stochastic nature of the machining processes of brittle materials. The first step to gain more information about the machining process is the realization of single grain wear tests on different natural stone slabs and cement.

A. Experimental Setup

To gain information about the fundamental correlations between process parameters and workpiece specifications, single grain scratch tests have been accomplished. Within these, isolated diamond grains, brazed on steel pikes have been manufactured (see Fig 1) to prevent side effects from the binder phase or forerun diamond scratches as they occur in the grinding segments in real life application. To provide consistent workpiece properties high strength concrete specimens of specification DIN 1045-1, C80/90 containing basalt as the only aggregate had been produced. Besides these the two phases, cement binder and basalt were separately prepared as homogeneous specimens for an analysis of the material specific influence on the wear.

To eliminate further side effects such as hydrodynamic lubrication, interaction of previously removed material and adhesion, the experiments have been carried out without any coolant. The brazed diamond pikes had been attached to a rotating disc which in turn had been mounted to the machine (see Fig. 2) to simulate the original process kinematic. Parameters for the experimental design were chosen according to common tools and trepanning processes. To guarantee constant depth of cut the rotatory motion of the diamond pike had been superimposed by a constant feed which generated a

Manuscript received June 28, 2011.

[1]TU Dortmund University, Faculty of Statistics, Dortmund, Germany
[2]TU Dortmund University, Institute of Machining Technology, Dortmund, Germany
[3]TU Dortmund University, Institute of Materials Engineering, Dortmund, Germany

ISBN: 978-988-19251-7-6
ISSN: 2078-0958 (Print); ISSN: 2078-0966 (Online)

Fig. 1. Sample Before and After Brazing.

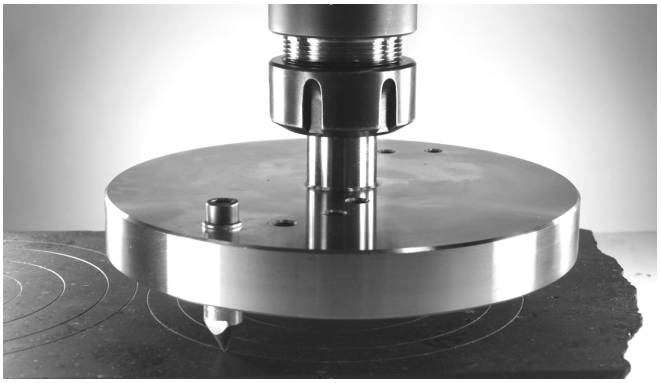

Fig. 2. Scratch Test Device on Basalt.

helical trajectory. To generate a measureable diamond wear, a certain distance had to be accomplished. Therefore a total depth of cut of 250 μm had been achieved in every test.

II. Simulation Model

The general aim of the project at hand is the optimization of the machining process w.r.t. production time, forces affecting the workpiece and tool wear. For this aim knowledge about the relationships between adjustable process parameters, measurable covariates and the outcome is inevitable. Then optimal strategies and parameter settings can be derived from this knowledge. As the real machining experiments are very time consuming and expensive it is of primary interest to develop a realistic simulation model. This model then can be used for the derivation and testing of such strategies and settings before verification in real processes.

Many proposals for the simulation of grinding processes had been made in the past, see e.g. [3] and [8] for overviews. These proposals in general are combinations of models of temperature, energy, topography, wear and forces. While the common approaches model the topography of tool and workpiece on regular grids, in our work we consider both the diamond grain and the workpiece as a complete tessellation of stochastically distributed microparts. The connections of these microparts are seen as predetermined breaking points, at which chip removals and break-outs will occur. As microfracture is the dominant wear mechanism in grinding (see [9]) and due to the abrasivity of the considered materials this point of view seems more straightforward and suitable for the process under study.

With the tessellations of grain and workpiece a geometric simulation is then performed where the affecting forces in each simulation step are determined in dependance of the sizes and shapes of the intersecting microparts. By doing so

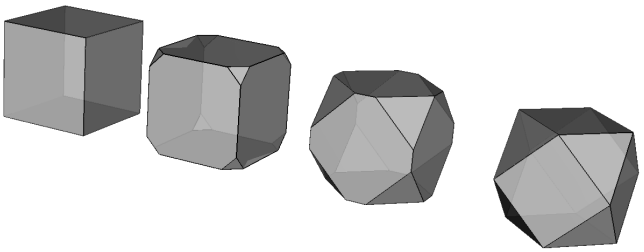

Fig. 3. Different Diamond Grain Shapes.

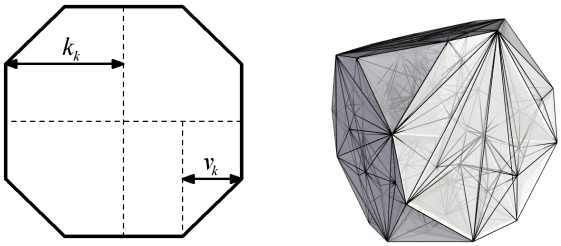

(a) (b)

Fig. 4. Edge Lengths and Reductions (a) and Delaunay Tessellation (b) of Simulated Diamond Grain.

- in contrast to the usual way of static force computation based an phenomenological equations and assuming fixed force ratios - time series of the forces can be simulated directly and validated and calibrated by fitting the model parameters statistically to a series of real experiments.

A. Modeling of Diamond Grain and Workpiece

The Modeling of the diamond grain is obtained by first determining its vertices by assigning the values of two parameters controlling for size and shape of the grain. There the shape of the grain is assumed to be given by the 14-sided body that is formed when the corners of a cube are flattened (see Fig. 3).

The first parameter k_k specifies the half of the cube's edge length in mm, while the parameter v_k is given by the reduction of the edge length resulting of the flattening of each corner (see Fig. 4a).

Within the modeling the grain is assumed to consist of microparts which may flatten or disrupt during the machining process. For simplicity it is further assumed, that these microparts have the shapes of simplices. The corresponding grain structure is simulated by randomly generating $n_{p;k}$ points in the interior of the grain and then computing the three-dimensional Delaunay Tessellation (see [2]) of the union of these points and the diamond's vertices (see Fig. 4b). Beside $n_{p;k}$ the statistical distribution of the points has to be specified, where all following results are based on the uniform distribution.

The workpiece is modelled equivalently, while the simplices in this case state the chips cutted from the material during the machining process. As for the chips higher volumes can be assumed than for the microparts of the diamond, the vertex density has to be set correspondingly lower. In the single grain scratch experiments under consideration exclusively circular scratch paths have been produced. Hence the workpiece is reduced to a ring covering the produced scratch path due to computation time. The workpiece's geometry is

ISBN: 978-988-19251-7-6
ISSN: 2078-0958 (Print); ISSN: 2078-0966 (Online)

correspondingly fully described by the parameters inner and outer diameter $d_{i;w}$ and $d_{a;w}$ and it's height h_w. The numbers $n_{s;k}$ and $n_{s;w}$ of diamond and workpiece simplices can not in general be derived from the point numbers $n_{p;k}$ and $n_{p;w}$ but depend on the specific tessellations.

B. Process Simulation

The position of the workpiece stays constant during the whole process and lies centered around the origin parallel to the xy-plane, where the lower side is marked by $z = 0$. The 2.5-fold of the diamond edge length is assigned to the ring width, so with drilling diameter d_p inner and outer diameter compute to $d_{i;w} = d_p - 2.5k_k$ and $d_{i;w} = d_p + 2.5k_k$. For the determination of the grain it is first centered around the origin in all dimensions and successively turned around all axes by the angels α_x, α_z and α_y, which changes the $n_k = n_{p;k} + 24$ grain vertices $S_k \in I\!R^{n_k \times 3}$ to

$$S'_k = S_k R_x R_z R_y \text{ with } R_x = \begin{pmatrix} 1 & 0 & 0 \\ 0 & cos\alpha_x & -sin\alpha_x \\ 0 & sin\alpha_x & cos\alpha_x \end{pmatrix},$$

$$R_z = \begin{pmatrix} cos\alpha_z & 0 & sin\alpha_z \\ 0 & 1 & 0 \\ -sin\alpha_z & 0 & cos\alpha_z \end{pmatrix}, R_y = \begin{pmatrix} cos\alpha_y & -sin\alpha_y & 0 \\ sin\alpha_y & cos\alpha_y & 0 \\ 0 & 0 & 1 \end{pmatrix}.$$

The grain is finally moved to its starting position by shifting all grain vertices along the x-axis by d_p and along the z-axis by the starting height $h_{k;0}$:

$$S^0_k = \begin{pmatrix} s'_{k11} + d_p & s'_{k12} + h_{k;0} & s'_{k13} \\ \vdots & \vdots & \vdots \\ s'_{kn_k1} + d_p & s'_{kn_k2} + h_{k;0} & s'_{kn_k3} \end{pmatrix}.$$

Beside d_p in mm the depth of cut a_p in $\mu m/r$ and the cutting speed v_p in rpm form the process parameters. With sample rate r_p in Hz at the beginning of each iteration i the actual position of the grain can be determined by turning the grain vertices around the z-axis and shifting them along the same axis:

$$S^i_k = S^{i-1}_k \begin{pmatrix} cos\alpha_r & 0 & sin\alpha_r \\ 0 & 1 & 0 \\ -sin\alpha_r & 0 & cos\alpha_r \end{pmatrix} - \begin{pmatrix} 0 & a_r & 0 \\ \vdots & \vdots & \vdots \\ 0 & a_r & 0 \end{pmatrix}$$

with $\alpha_r = (2\pi v_p)/(60 r_p)$, $a_r = (a_p v_p)/(60000 r_p)$.

Next in each iteration the matrix W_s of intersection volumes of all pairs of grain and workpiece simplices is computed, where the (l, j)th entry of W_s reflects the intersection volume of the lth grain simplex with the jth workpiece simplex.

C. Workpiece Affecting Forces

In the following for each workpiece simplex intersecting at least one grain simplex it is determined, which force affects it. For this purpose first the total mass $m_{k;j} = \sum_{l:w_{s;lj}>0} w_{k;l}\rho_k$ of all grain simplices that intersect the actual workpiece simplex j is computed from the grain simplex volumes $w_{k;l}$ and the diamond density ρ_k. By interpreting the collision of workpiece and grain simplices as a force impact the force affecting the jth workpiece simplex can be simulated by assuming the relation $F_{ij} = (v_p m_{k;j})/t_d$, where the constant t_d is another parameter of the simulation model.

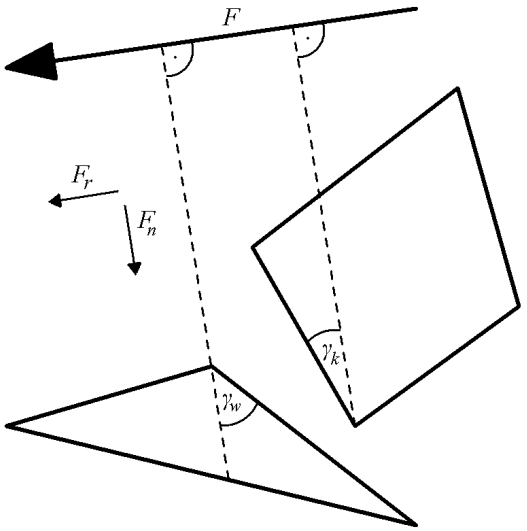

Fig. 5. Geometric Distribution of Forces on Collision of Grain and Workpiece Simplex.

How the workpiece affecting force F_{ij} distributes in radial and normal direction depends on the geometrical properties of the involved simplices. In this context for simplicity only the largest grain simplex is considered and the vertices of this simplex as well as those of the workpiece simplex are projected to the vertical plane parallel to the cutting direction. In this projection the angle γ_k between the vector orthogonal to the cutting direction and that vertex of the grain simplex, that contacts the workpiece simplex first, is computed. After determining the corresponding angle γ_w the normal and radial forces can be computed by $F_{n;ij} = F_{ij} sin[max(\gamma_w, \gamma_k)]$ and $F_{r;ij} = F_{ij} cos[max(\gamma_w, \gamma_k)]$ (see Fig. 5).

The total forces affecting the workpiece in iteration i are then given by

$$F_{n;i} = \sum_{j:\sum_{l=1}^{n_{s;k}} w_{s;lj}>0} F_{n;ij} \text{ and } F_{r;i} = \sum_{j:\sum_{l=1}^{n_{s;k}} w_{s;lj}>0} F_{r;ij}.$$

D. Tool Wear

In general due to the high grade of the diamond it can be assumed, that the actual workpiece always loosens from its bond. But since according to experience also disruptions of the diamond occur it is further assumed, that the involved diamond simplices break out, whenever the mass of the hit workpiece simplex exceed their own mass by a specific factor μ_k, i.e. when the inequality $w_{w;j}\rho_w > \mu_k m_{k;j}$ holds. If the inequality condition is not fulfilled the diamond simplices are supposed to continuously flatten, which is simulated by shifting the vertex closest to the workpiece towards the opposite triangle in orthogonal direction by a specific percentage η_k.

The material removal rate of the workpiece and the wear rate of the diamond at the end of each iteration is then given

ISBN: 978-988-19251-7-6
ISSN: 2078-0958 (Print); ISSN: 2078-0966 (Online)

Fig. 6. Simulated Machined Workpiece and Diamond Grain.

compute (S_k, S_w)
$S_k^0 \leftarrow S_k R_x R_z R_y + (d_p, h_k, 0) \otimes 1_{n_k}$
for $i = 1 \rightarrow i_{max}$ **do**
  $S_k^i \leftarrow S_k^{i-1} R_r - (0, a_r, 0) \otimes 1_{n_k}$
  compute intersection volumes W_s
  for $j = 1 \rightarrow n_w$ **do**
    $m_{k;j} \leftarrow \sum_{l:w_{s;lj}>0} w_{k;l}\rho_k$
    compute (γ_w, γ_k)
    $\gamma \leftarrow max(\gamma_w, \gamma_k)$
    $F_{ij} \leftarrow (v_p m_{k;j})/t_d$
    $(F_{n;ij}, F_{r;ij}) \leftarrow F_{ij}(sin\gamma, cos\gamma)$
    if $w_{w;j}\rho_w > \mu_k m_{k;j}$ **then**
      remove diamond simplices $l : w_{s;lj} > 0$
    else
      reduce heights of diamond
        simplices $l : w_{s;lj} > 0$ by η_k
    end if
    remove workpiece simplex j
  end for
  $(F_{n;i}, F_{r;i}) \leftarrow (\sum_j F_{n;ij}, \sum_j F_{r;ij})$
end for

Fig. 7. Pseudocode Representation of Simulation Model.

by the change of the corresponding volumes. Figure 6 shows an exemplary view of a machined workpiece and a diamond grain, for better visualization in unrealistic proportions.

Figure 7 shows a pseudocode representation of the proposed simulation model.

E. Model Fitting

For the estimation of the unknown model parameters the results of a series of 93 single grain scratch experiments are available. The series was planned by a statistical Design of Experiments, where the process parameters v_p, a_p and d_p have been varied. Table I contains the used levels of these factors. Because the diameter d_p is not adjustable continuously, a Central Composite Design (CCD) of v_p and a_p had been repeated for each of the four diameter levels. By means of a stepwise forward-backward-selection based on the Akaike Information Criterion ([1]) taking into account linear, quadratic and two-fold interaction effects of the process parameters on the averaged forces the following models could be derived:

TABLE I
FACTOR LEVELS OF THE CCD

Factor	Levels				
d_p	50	80	110	130	
a_p	3.75	5	7.5	10	11.25
v_p	346	525	900	1275	1454

TABLE II
PREDEFINED AND FIXED PARAMETERS OF THE SIMULATION MODEL

Parameter	Status	Value
r_p	Predefined	10000
ρ_w, ρ_k	Predefined	2, 3.52
k_k, v_k	Predefined	1, 0.7
α_x, α_z, α_y	Predefined	$\pi/4$, $\pi/4$, $\pi/4$
$n_{p;w}/mm^3$	Fixed	10
$n_{p;k}/mm^3$	Fixed	500

TABLE III
FACTOR LEVELS OF THE 3^3-DESIGN

Factor	Levels		
μ_k	5	15	25
η_k	0.01	0.025	0.04
t_d	10	55	100

$$\hat{\bar{F}}_n = 44.025 - 0.524 d_p - 0.351 a_p^2 + 0.062 d_p a_p$$
$$\hat{\bar{F}}_r = -5.204 + 0.007 v_p + 2.425 a_p - 0.187 a_p^2 - 0.00009 v_p d_p + 0.007 d_p a_p.$$

The regressors of these models are all significant on a level of 5%, the R^2s are 0.181 and 0.236. The low goodness of fit has to be seen in the context of the relatively high reproduction variance, due to which the R^2 values are limited by 0.652 and 0.628.
The fit of the simulation model was obtained by minimizing the quadratic deviations of simulated and measured forces in dependance of the model parameter μ_k, η_k and t_d. Table II lists the remaining parameters, which can be derived from the geometrical and physical properties of tool and workpiece or had been fixed.

For the determination of the parameter values a two-step procedure is chosen. First a full factorial 3^3-Design (see table III) for the model parameters is constructed and replicated for each of the process parameter settings of the cube of the CCD. Following this combined design in total $33 \cdot 23 = 216$ experiments are simulated. Next a quadratic model of the squared force deviation in dependance of the model parameters is fitted. By minimizing the corresponding model equation the model parameters are estimated by $\mu_k = 10.638$, $\eta_k = 0.036$ and $t_d = 39.8$.

In the second step, the model calibration, process parameter dependant scale terms $s_r(v_p, a_p, d_p)$ and $s_N(v_p, a_p, d_p)$ are introduced to adjust the remaining systematic model deviations. These scale terms represent the mean ratios between modelled and simulated forces $F_{r;M}/F_{r;S}$ and $F_{n;M}/F_{n;S}$ and are obtained by fitting the models $F_{r;M}/F_{r;S} = (v_p, a_p, d_p)\beta_r + \epsilon_r$ and $F_{n;M}/F_{n;S} = (v_p, a_p, d_p)\beta_n + \epsilon_n$.

ISBN: 978-988-19251-7-6
ISSN: 2078-0958 (Print); ISSN: 2078-0966 (Online)

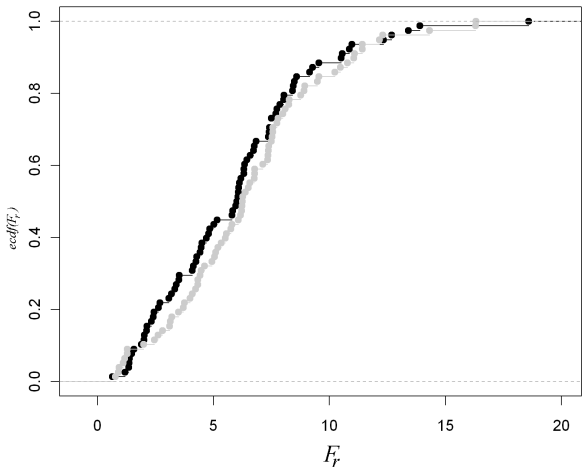

Fig. 8. Comparison of the Empirical Distribution Functions of Measured (Black) and Simulated (Gray) Radial Forces.

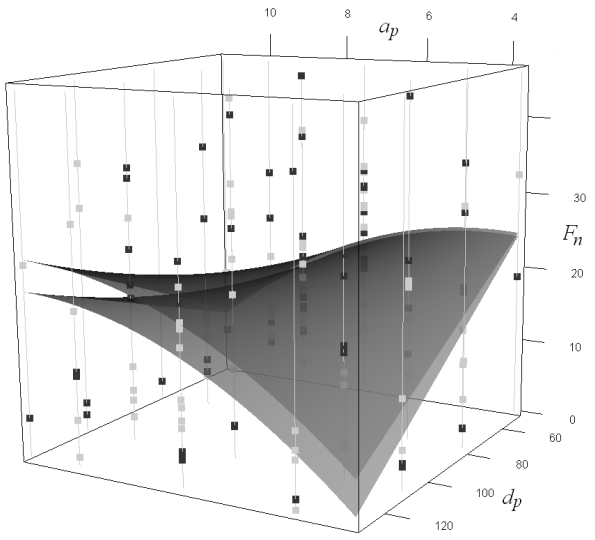

Fig. 9. Response Surfaces of the Regression Models for F_n Based on Measured (Lower Surface) and Simulated (Upper Surface) Data and Measured (Gray) and Simulated (Black) Data Points.

The application of the calibrated model is performed by first applying the simulation model with known, predefined and estimated parameter values and then multiplying the resulting force time series by the scale terms.

F. Results

Following the procedure described in the last section for each row of the CCD a process had been simulated. The comparison between the empirical distribution functions of measured and simulated forces do not show severe differences, as can be seen in Figure 8 at the example of F_r.

For further evaluation of the results the force regression models based on measurements and simulations are compared, where the nominal regressors are provided by the fit to the real data. Figure 9 shows a visual comparison of the results for F_n.

Apparently both response surfaces are very close to each other and simulated and measured data vary in comparable ranges. A similar picture can be generated for F_r. To decide,

TABLE IV
RESULTS OF THE JOINT REGRESSION MODELS OF SIMULATED AND MEASURED FORCE DATA. COEFFICIENTS SIGNIFICANT ON A LEVEL OF 5% BOLD.

	Model for F_n		Model for F_r	
Regressor	Coefficient	p-Value	Coefficient	p-Value
$Intercept$	**42.666**	**<0.0001**	**-9.184**	**0.0031**
v_p			**0.0055**	**0.0079**
a_p			**3.671**	**<0.0001**
d_p	**-0.4934**	**0.0003**		
a_p^2	**-0.3399**	**0.0018**	**-0.253**	**<0.0001**
$v_p d_p$			**-0.00006**	**0.01**
$a_p d_p$	**0.0599**	**0.0005**	0.00406	0.106
I_F	-1.0435	0.8868	-2.956	0.3358
$I_F v_p$			-0.00254	0.2277
$I_F a_p$			1.048	0.2143
$I_F d_p$	0.02635	0.8419		
$I_F a_p^2$	0.0027	0.9801	-0.0587	0.3413
$I_F v_p d_p$			0.000035	0.102
$I_F a_p d_p$	-0.00048	0.9774	-0.00031	0.2114

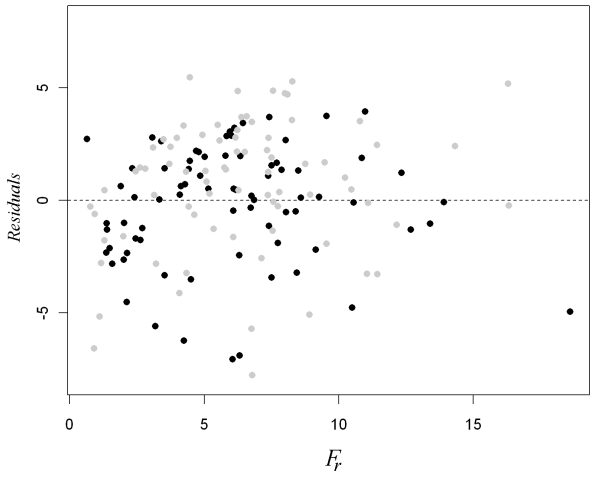

Fig. 10. Comparison of Cross-Over Residuals for F_r Based on Measured (Gray) and Simulated (Black) Data.

whether the differences between the models are significant, joint models for simulated and measured forces are fitted. For these models, an indicator variable I_F measuring if a specific data point had been measured ($I_F = -1$) or simulated ($I_F = +1$) is introduced. The variable I_F is included into the joint models as well in main effect as in interaction with all contained regressors. The results of these joint models are shown in table IV.

Obviously the influence of I_F in both models is neither in main effect nor in any interaction significant. This results confirms the assumption, that for both simulated and measured forces the same models hold.

Finally the residuals of the regression models are investigated. There the residuals are determined cross-over by computing the deviations between the predictions for the measured forces based on the model of the simulated data and vice versa. Figure 10 shows the residuals for F_r, for F_n a similar picture can be obtained.

ISBN: 978-988-19251-7-6
ISSN: 2078-0958 (Print); ISSN: 2078-0966 (Online)

The residuals neither show a structure along the corresponding dependant variable nor any systematic differences between the residuals based on simulations and measurements can be seen.

So it can be stated that the forces obtained by simulations as intended show a similar behavior as the real force data, so that the model can be assumed to be adequate for further application in the closer investigation of the machining process.

III. Conclusion

By the proposed simulation model based on Delaunay Tessellations of diamond grain and workpiece an efficient, flexible and valid method for the determination of the material removal rate, the tool's wear and the forces affecting the workpiece with given process parameters has been introduced.

In the next project phases this model will be successively extended for the application in multi-grain and multi-phase concrete machining processes. Therefore the grain orientation that has been kept constant during this work will be explicitly taken into account as a covariate within the fitting procedure. Furthermore the heterogeneity of the material will be modelled by allowing for local variation of the properties of the workpiece simplices. All model extensions will be accompanied by validations and calibrations based on statistical designs of experiments. The application in practice then will be the opportunity to derive the best process parameter settings as well as grain type, size and density in specific situations where typically workpiece material and hole diameter are given and to quantify uncertainty by giving interval estimators for the interesting outcome.

Acknowledgment

This work has been supported in part by the Collaborative Research Center Statistical Modelling of Nonlinear Dynamic Processes (SFB 823) of the German Research Foundation (DFG), within the framework of Project B4, Statistical Process Modelling for Machining of Inhomogeneous Mineral Subsoil.

References

[1] H. Akaike, "A new look at the statistical model identification," in *IEEE Transaction on Automatic Control*, vol. 19, pp. 716-723, 1974.

[2] C. B. Barber, D. P. Dobkin, and H. T. Huhdanpaa "The Quickhull algorithm for convex hulls," in *ACM Trans. on Mathematical Software*, vol. 22, no. 4, pp. 469-483, 1996.

[3] E. Brinksmeier, J. C. Aurich, E. Govekar, C. Heinzel, H.-W. Hoffmeister, J. Peters, R. Rentsch, D. J. Stephenson, E. Uhlmann, K. Weinert, and M. Wittmann "Advances in Modeling and Simulation of Grinding Processes," in *Annals of the CIRP: Manufacturing Technology*, vol. 55, no. 2, pp. 667-696, 2006.

[4] B. Brook "Principles of Diamond Tool Technology for Sawing Rock," in *Int. J. Rock Mechanics & Mining Sciences*, vol. 39, no. 1, pp. 41-58, 2002.

[5] B. Denkena, D. Boehnke, B. Konopatzki, J.-C. Buhl, S. Rahman, and L. Robben "Sonic analysis in cut-off grinding of concrete," in *Production Engineering*, vol. 2, no. 2, pp. 209218, 2008.

[6] J. D. Dwan, 'Production of Diamond Impregnated Cutting Tools," in *Powder Metallurgy*, vol. 41, no. 2, pp. 84-86, 1998.

[7] J. Konstanty, and A. Bunsch "Hot Pressing of Cobalt Powders," in *Powder Metallurgy*, vol. 34, no. 3, pp. 195-198, 1991.

[8] H. K. Tönshoff, J. Peters, I. Inasaki, and T. Paul "Modelling and Simulation of Grinding Processes," in *Annals of the CIRP: Manufacturing Technology*, vol. 41, no. 2, pp. 677-688, 1992.

[9] F. W. Pinto, G. E. Vargas, K. Wegener "Simulation for optimizing grain pattern on Engineered Grinding Tools," in *Annals of the CIRP: Manufacturing Technology*, vol. 57, no. 1, pp. 353-356, 2008.

ISBN: 978-988-19251-7-6
ISSN: 2078-0958 (Print); ISSN: 2078-0966 (Online)